Eur. Phys. J. D **22**, 217–227 (2003)
DOI: 10.1140/epjd/e2003-00014-0

THE EUROPEAN PHYSICAL JOURNAL D

A correlation study of small silver clusters

M.N. Huda and A.K. Ray[a]

Department of Physics, The University of Texas at Arlington, P.O. Box 19059, Arlington, Texas 76019, USA

Received 16 April 2002 / Received in final form 12 September 2002
Published online 21 January 2003 –

Abstract. The formalisms of many body perturbation theory and coupled cluster theory have been used to study the electronic and geometric structures of neutral, cationic, and anionic small silver clusters. Hay-Wadt relativistic effective core potentials replacing the twenty-eight core electrons and a Gaussian basis set have been used. Topologically different clusters and clusters belonging to different symmetry groups have been identified and studied in detail. Full geometry optimizations have been carried out at four different correlated levels of theories. Ionization potentials, electron affinities, and fragmentation energies of the optimized clusters have been compared with other experimental and theoretical results available in the literature. No convergence problems are encountered at the various levels of correlated theories. This is noteworthy since it has been claimed in the literature that for d elements the MP series does not converge very well.

PACS. 71.15.Nc Total energy and cohesive energy calculations – 73.22.-f Electronic structure of nanoscale materials: clusters, nanoparticles, nanotubes, and nanocrystals

1 Introduction

Clusters are distinctly different from their bulk-state, and exhibit many specific properties, which distinguishes their studies as a completely different branch of science named "Cluster Science". Ideas like "super-atoms", "magic numbers" or "fission" in clusters [1–3] provokes a wider class of scientists to study this "relatively" new area of the physical sciences. Growing interest in the stabilities of small clusters and the evolution of bulk properties from cluster properties is also due to the emergence of a new science called nanoscience and its potential in industrial applications. Moreover, a complete understanding of the physics of clusters, employing different theoretical models, is itself a demanding topic in many body physics. In the study of metal clusters, silver has received particular attention because of two reasons: one is theoretical in that the silver has d-electrons at the outer orbitals, overlapped by the partially filled s-orbitals, which makes the study of silver clusters interesting and challenging; the second one is applied because of the importance of silver in photographic and catalytic processes [4].

There is, in fact, a recent growth of experimental work concerning different aspects of silver clusters [5–13]. Spasov *et al.* [14] used energy-resolved collision-induced dissociation (CID) method to study fragmentation patterns, cross-sections, and dissociation energies of anionic silver clusters (Ag_n^-, $n = 2$–11). The main reaction channels were found to be the loss of an atom and also the loss of a dimer, with the dimer less favored for odd n values. The dissociation energies for the loss of an atom showed strong odd-even alternation. Photoelectron spectra of silver clusters were studied by Handschuh *et al.* [15] at different photon energies to explore the electronic structures of individual clusters. They observed sharper spectral patterns of Ag clusters than the corresponding alkali metal clusters which, according to the authors, might be due to the stronger bonding in silver clusters. This can be interpreted as the result of overlapping of the outer d and s orbitals, which gives rise to van der Waals type attractive force. Femtosecond NeNePo (negative to neutral to positive) spectroscopy was used to study the structural dynamics of Ag_3 clusters [16], and the wave packet dynamics along the coordinate of the linear-to-triangular rearrangement on the ground state potential surface was reported in details by Boo *et al.* [17]. The authors also commented about breaking of the degeneracy of the neutral Ag_3 state due to strong Jahn-Teller effect.

Between the two possible valence electronic configuration $^2\mathrm{D}(4d^9 5s^2)$ and $^2\mathrm{S}(4d^{10}5s^1)$, we found the former state to be at 4.22 eV higher than the latter one at the fourth-order many-body perturbation theory level (MP4) of calculation and the $^2\mathrm{P}(4d^{10}5p^1)$ state at 3.28 eV higher. Though the chemistry is primarily due to the valence s-electrons, the electronic properties and the stability of the clusters are strongly dominated by the filled d-electrons screening the oscillator strength of valence electrons [18]. As pointed out by Luh *et al.* [19] in their studies of d-band quantum well states, the d-electrons have more localized wave functions and experience a larger correlation effect and have smaller energy dispersions and group velocities, for silver $4d$ shell is almost like a shallow core-level. Moreover, d and outer s valence electron correlation

[a] e-mail: akr@uta.edu

is responsible for the long-range attractive van der Waals type interaction [20]. Some authors have commented that s–d interaction might not be well handled by perturbation methods [21,22] and one purpose of this work is to test this hypothesis for small silver clusters. Methods have been also developed to deal s–d hybridization based on the second moment approximation of the electron density of states in a tight binding model, called the Gupta model [23–25]. An extensive study for large silver clusters using this model has been carried out by Michaelin *et al.* [26].

Despite the obvious importance of d-shell in silver cluster binding, some work has been done taking $4d$ orbitals inside the core potential and treating s as the only active valence electron as in the case of alkali metal clusters [27,28]. This approach may be useful to study the qualitative features of the silver clusters, but, as pointed out by the authors, may not be suitable for exact determination of the properties of silver clusters. An experimental study [29] did comment that majority of spectroscopic phenomena can be explained in terms of s electrons. This statement is incomplete in the sense that, unlike alkali metal clusters, where resonance frequency decreases with the cluster size, a phenomenon called "red-shift", cationic silver clusters show "blue-shift", which means in this case resonance frequency increases with decreasing cluster size. This event can only be explained in terms of d electrons. Density functional theory (DFT) has also been employed in conjunction with pseudopotentials to study silver clusters [30–32] and the dynamics of internal motion in silver clusters [33]. Kaplan *et al.* [30] used an all-electron spin density approach with nonlocal corrections and a contracted [$6s5p3d$] basis set for the molecular orbitals to study neutral and anionic silver clusters up to the hexamer. To the contrary of the case of tetramers and pentamers, they found that anionic and neutral hexamers have different stable geometries. Poteau *et al.* [31] performed DFT calculations with the use of a 19e RECP combined with the BP86 functional and a [$3s3p4d$] basis set. Fournier [32] used Kohn-Sham density functional theory with a 17 electron pseudopotential and a contracted [$3s3p1d$] basis set for a detailed study of neutral silver clusters. Local spin density (LSD) approximation implemented *via* the Vosko-Wilk-Nusair (VWN) exchange correlation functional was used and the two degenerate states of Ag_3, namely $^2B_2$ and $^2A_1$, were found to have an energy difference of more than 0.18 eV, contradicting some of the earlier works (see *e.g.* Ref. [17] and references therein) and also our work as detailed below. Liu *et al.* [33] studied the stability and internal motion in Ag_n (n = 4–6) clusters, with *ab initio* molecular dynamics methods, based on density functional theory with plane waves and pseudopotentials. Work has also been done, treating the $4d$ electrons along with the $5s$ electrons as valence electrons, with all the others treated as core electrons [34–36].

In reference [35], a new 11-electron relativistic effective core potential (11e-RECP) was proposed, based on the 11e-RECP of Hay and Wadt [37]. The parameters were optimized by root-mean-square minimization of various properties of the silver atom and the dimer with respect to experimental data and naturally, the results were in very good agreement with experimental data. The basis set used was a contracted [$5s3p2d$] set and the theoretical methods used were the multi-reference doubles configuration interaction (MRD-CI) and coupled cluster singles and doubles (CCSD) techniques. On the other hand, Ramirez-Solis *et al.* [38], using CASSCF+CASPT2 and CCSD (T) methods, showed that this 11e-RECP produces transition energies very far from the experimental values. Jarvis *et al.* [39] used *ab initio* molecular dynamics (AIMD) for the analysis of vertical excited states along ground state trajectories of Ag_3. They also performed a relative comparison of the various RECPs. At sample low-temperature neutral trajectories, the 11e-RECP of reference [35] showed more reluctance to produce bending, bending only about $\sim$35° from the linear structure. In contrast, Hay-Wadt's 11e-RECP gave a much wider range of bending angles at low-temperature consistent with expected physical behavior. Zhao *et al.* [40] developed a tight-binding model to study the structural and electronic properties of sliver clusters. The ground state structures of Ag clusters containing up to 21 atoms were optimized by molecular dynamics based genetic algorithm.

To date, the smallest core used for sliver clusters is the 19e-RECP [4,19,41]. As the computational process is very expensive at this level even for small clusters, full geometry optimization results with different levels of post-HF theory have *not* been reported in the literature so far. In this work, we present results on neutral, cationic, and anionic silver clusters (Ag_n, n = 2, 3, 4) at four different theory levels, namely second-order perturbation theory (MP2) [42], fourth-order perturbation theory (MP4) [43], coupled-cluster-singles-doubles (CCSD) and coupled-cluster-singles-doubles-triples (CCSDT) levels [44]. Complete geometry optimizations at different possible spin configurations have been performed at each level, and the results at different levels have been compared.

2 Computational methods and results

Both the many-body perturbation theory (MBPT) and coupled-cluster (CC) theory, as used in this work, are well documented in the literature [42–49]. Here we present some basic equations to define some terms. In MBPT, the energy is given by the linked diagram expansion

$$\Delta E = E - E_0 = E_1 + E_{\rm corr}$$
$$\Delta E = \sum_{n=0}^{\infty} \langle \Phi_0 | V[(E_0 - H_0)^{-1} V]^n | \Phi_0 \rangle_L \qquad (1)$$

where $|\Phi_0\rangle$ is taken to be the UHF wave functions, H_0 is the sum of one-electron Fock operators, E_0 is the sum of the UHF orbital energies, and $V = H - H_0$, is the perturbation with H the usual electrostatic Hamiltonian. The subscript L indicates the limitation to linked diagrams. Though one can include various categories of infinite-order

Table 1. Ionization potentials, electron affinities and transition energies (in eV) of the Ag atom.

Method	IP	EA	$^2S \rightarrow {}^2P$	$^2S \rightarrow {}^2D$
MP2	6.603(5.794)[a]	0.268(0.144)	3.260	4.420
MP4	6.664(5.816)	0.579(0.494)	3.281	4.221
CCSD	6.626(5.814)	0.548(0.255)	3.239	4.091
CCSD (T)	6.654(5.825)	0.607(0.466)	3.251	4.128
Exp. [51]	7.576	1.302	3.740	3.970

[a]Values in bracket are all-electron values calculated with 3-21G** basis set.

summations from equation (1), the method is usually limited by termination at some order of the perturbation theory. For the Ag clusters, we have carried out second order (MP2) and complete fourth-order calculations (MP4), which consist of all single-, double-, triple- and quadruple-excitation terms.

In coupled cluster method, the exact wave function $|\Psi\rangle$ of an N-electron system is written as follows:

$$|\Psi\rangle = \mathrm{e}^T |\Phi_0\rangle \tag{2}$$

where the cluster operator T is defined as a sum of its many-body components

$$T = \sum_{i=1}^{N} T_i,$$

and $|\Phi_0\rangle$ is usually Hartree-Fock determinant. In approximate CC theory, the sum is truncated at some point. For CCSD we have $T = T_1 + T_2$ and for CCSDT we go up to $i = 3$. CCSDT method has an eighth-order dependence on the size of the system and as such is computationally too expensive to apply. So a non-iterative treatment of triple excitations was introduced, which is now generally known as CCSD (T).

As indicated before, the general approach to study silver clusters has been to use effective core potentials (pseudopotentials). Though ECPs reduce computational times and one can incorporate the relativistic effect on the inner electrons, there is a tendency to overestimate the bond-length and underestimate the dissociation energy. However, such errors could be minimized by choosing small core pseudopotentials and this is particularly necessary for silver clusters since the d-electrons play very important roles. We have used the Hay and Wadt [50] 19e **R**elativistic **E**ffective **C**ore **P**otential (19e-RECP). In this core potential the inner 28 electrons ($1s^2\,2s^2\,2p^6 3s^2\,3p^6\,3d^{10}$) are replaced by RECP and the outer 19 electrons ($4s^2\,4p^6\,4d^{10}\,5s^1$) are taken as valence electrons. The mass-velocity and Darwin relativistic effects have been incorporated in the potentials and a [3s3p2d] Gaussian basis set has been used. To estimate the accuracy of this RECP at different levels of theory, we compare in Table 1 the atomic silver ionization potentials (IP) and electron affinities (EA) obtained with this 19e-RECP, with the all electron 3-21G** basis set [49] results and with experimental results. The values obtained with the RECP are certainly closer to the experimental results than the all-electron results. However, in as much as the IPs at the various levels of theory differ from the experimental value by about twelve percent, the electron affinity even at the CCSD (T) level is only about half of the experimental value [51]. We also computed two transition energies, namely $^2S(4d^{10}5s^1) \rightarrow {}^2P(4d^{10}5p^1)$ and $^2S(4d^{10}5s^1) \rightarrow {}^2D(4d^9 5s^2)$ for the Ag atom and compared them with experimental values. The transition energies are found to be fairly close to the experimental values, varying between three percent and thirteen percent. The Gaussian 98 suite of programs [52] was used to perform the above and all the subsequent computations on a 16-processor SGI/Cray Origin 2000 supercomputer at the University of Texas at Arlington.

In the results to follow, the binding energies are computed from

$$E_b/n = (nE_1 - E_n)/n, \tag{3a}$$

where E_1 and E_n are the total energies of a silver atom and of the cluster, respectively.

For ionic clusters we use

$$E_b/n = (E_1^{\pm} + (n-1)E_1 - E_n^{\pm})/n, \tag{3b}$$

where $E_1^{\pm}$ and $E_n^{\pm}$ are the total energies of the ionic silver atom and of the cluster respectively.

We also computed the adiabatic and vertical ionization potentials (AIP and VIP respectively) by the following formula:

$$\mathrm{IP} = E_n^{+} - E_n, \tag{4}$$

where E_n^{+} is the total energy of the cationic clusters at the different levels of theory either at the cation optimized geometry (for AIP) or at the neutral geometry (for VIP). The electron affinities are calculated from

$$\mathrm{EA} = E_n - E_n^{-} \tag{5}$$

with E_n^{-} as the total energy of the geometry optimized anionic cluster.

Results for the neutral, cationic, and anionic silver dimers are presented in Tables 2, 3, and 4, respectively. The optimized clusters are also shown in Figure 1 and the binding energies per atom are presented in Figures 2–4. In as much as the literature on silver clusters is large, for the sake of brevity, we have compared our results with some representative DFT-based calculations [30–32], molecular dynamics based results [33,40], post-HF results [34,35,41] and of course, experimental results where available. Among the three DFT based calculations, we consider the results of Santamaria *et al.* [30] to be better because of the all-electron nature of the calculations and the size of the basis set. Similarly, for the post-HF based calculations, the results of Bauschlicher *et al.* [41] is judged to be better because of the small core 19-electron pseudopotential and a large contracted [5s4p4d1f] basis set. We hasten to point out that, given the different theoretical approaches used, this judgment is, to a large extent, qualitative in nature.

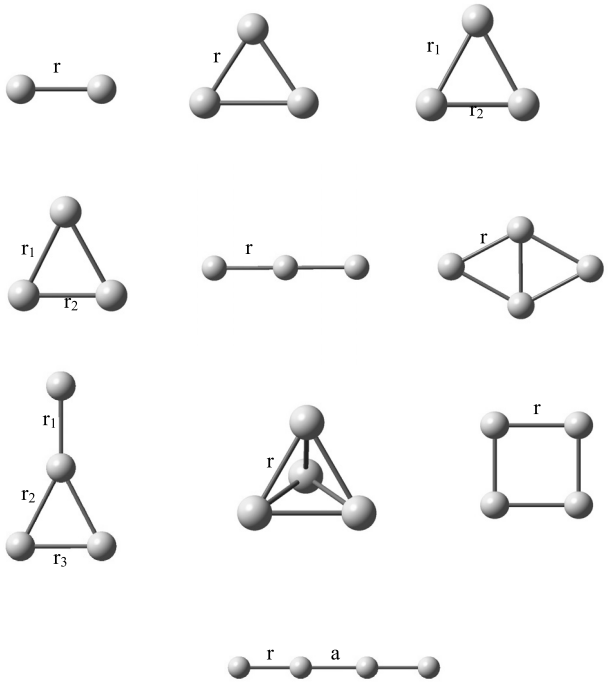

Fig. 1. Structures of silver clusters.

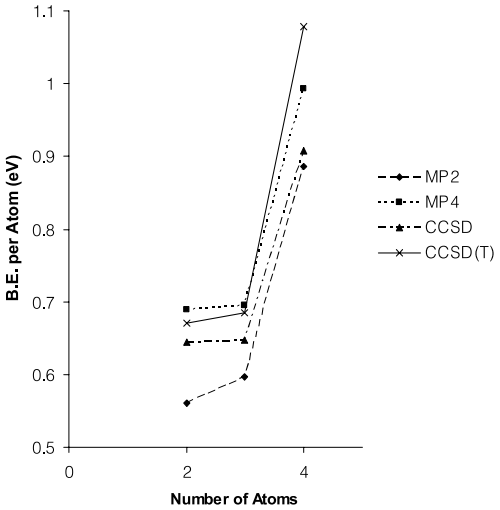

Fig. 2. Binding energies per atom for neutral Ag clusters *vs.* number of atoms in the cluster.

Table 2. $^1\Sigma_g^+$ ground state binding energies per atom, ionization potentials, electron affinities (all in eV) and bond lengths (in Å) for Ag_2.

Method	E_b/n	r	AIP	VIP	EA
MP2	0.561(0.700)[a]	2.681(2.631)	6.393	6.482	0.429
MP4	0.690(0.790)	2.681(2.629)	6.623	6.707	0.533
CCSD	0.645(0.770)	2.696(2.641)	6.512	6.587	0.613
CCSD (T)	0.671(0.800)	2.692(2.635)	6.581	6.658	0.657
Theory [30]	0.740	2.660		7.560	1.080
Theory [31]	0.860	2.570			
Theory [32]	1.11	2.504		8.580	
Theory [33]	0.892	2.574			
Theory [35]	0.910		7.180	7.260	...
Theory [41]	0.670	2.660	6.740	...	...
Exp.[b]	0.830	2.480	7.560		1.028 ± 0.01
Exp. [56]		...	7.600		

[a] Values in brackets are all-electron values calculated with 3-21G** basis set.
[b] These experimental values are quoted in reference [41].

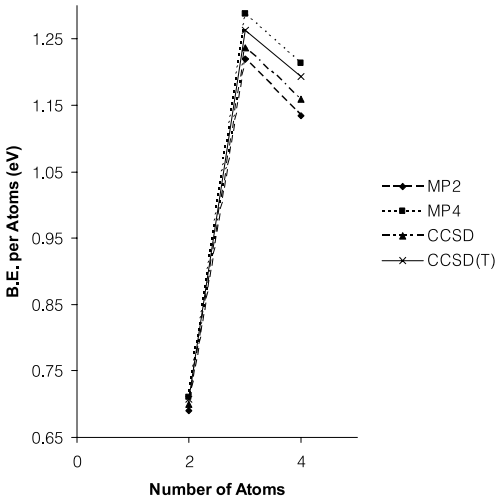

Fig. 3. Binding energies per atom for Ag cation clusters *vs.* number of atoms in the cluster.

Table 3. $^1\Sigma_g^+$ ground state binding energies per atom (in eV) and bond lengths (in Å) for Ag_2^+.

Method	E_b/n	r
MP2	0.690	2.910
MP4	0.710	2.900
CCSD	0.700	2.910
CCSD (T)	0.707	2.905
Theory [35]	0.870	2.690
Theory [41]	0.680	2.890

Table 4. $^1\Sigma_u^+$ ground state binding energies per atom (in eV) and bond lengths (in Å) Ag_2^-.

Method	E_b/n	r
MP2	0.670	2.820
MP4	0.660	2.900
CCSD	0.680	2.850
CCSD (T)	0.696	2.840
Theory [28]	0.760	2.754
Theory [30]		2.850
Theory [41]	0.560	2.810

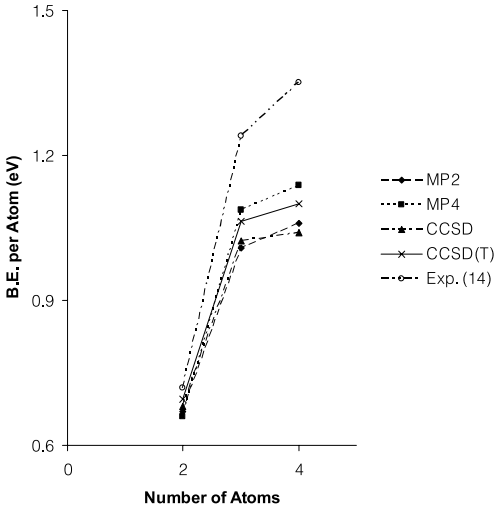

Fig. 4. Binding energies per atom for Ag anion clusters *vs.* number of atoms in the cluster.

For the neutral dimer with an electronic structure $...\pi_g^2\sigma_g^2$ producing a ground state $^1\Sigma_g$, results are also compared with all electron values computed with a 3-21G** basis set [49] in Table 2. At all levels of theory, the bond lengths computed with the RECP are higher than those computed with the all electron basis set and the binding energies are lower compared to all-electron values. On the other hand, the bond lengths are higher and the binding energies are lower at all levels of theory with both the RECP and the all electron basis set, compared to experimental values. The calculations of Bonacic-Koutecky *et al.* [35] and of Bauschlicher *et al.* [41] also report larger bond lengths compared to the experimental value but surprisingly, for binding energy, Bonacic-Koutecky *et al.* found a value higher than experimental binding energy. We also note that MP2 and MP4 level theories produced the same bond length. In the RECP calculations, the bond length is 2.68 Å and in the all electron calculation, the bond length is found to be 2.63 Å. However, the level of electron correlation, as expected, produced a significant difference in the values of the binding energy. For the cation, all four methods produced about the same bond length, significantly higher than the neutral dimer length. Same conclusions prevail for the binding energy. For the anionic dimer, the bond lengths are also larger compared to the neutral dimer, as expected from electron-electron repulsion and the binding energies are close to neutral binding energies. Our IP values differ with the experimental values from about 12.4 percent to about 15.9 percent at the various levels of theory.

For the neutral and charged (positive and negative) silver trimers, all possible structures were spin-optimized *i.e.* the geometries were optimized for different possible spin configurations. Results are presented in Tables 5, 6, and 7. Among the three possible geometrical structures for the neutral trimer, the isosceles structure was the most stable structure. Experimental evidence strongly suggests that the trimer is a Jahn-Teller distorted isosceles triangle. Based on our computations we find that there are two almost degenerate states: $^2B_2$ and $^2A_1$. The Mexican hat potential energy curves [17] demonstrate this feature. In fact, at the many body perturbation theory level, the difference in binding energies is only 0.001 eV at the MP2 level, while the two states are exactly degenerate at the MP4 level. The difference is 0.006 eV, both at the CCSD and at the CCSD (T) levels. The MP theories remain almost insensitive to the Jahn-Teller effect for the 19*e* RECP

Table 5. Binding energies per atom, ionization potentials, electron affinities (all in eV) and bond lengths (in Å) for different structures of neutral Ag_3.

Isosceles triangle $^2B_2$	E_b/n	r_1	r_2	AIP	VIP	EA
MP2	0.597	2.750	3.097	4.739	4.832	1.504
MP4	0.695	2.751	3.072	4.886	4.969	1.756
CCSD	0.648	2.778	3.149	4.858	4.958	1.673
CCSD (T)	0.685	2.774	3.124	4.920	5.011	1.742
Theory [30]						2.180
Theory [31]	0.840	2.627	3.028			
Theory [32]	0.861	2.56	2.900		6.340	
Theory [34]	0.900	2.720	2.871		5.900	
Theory [35]	0.980	2.580	2.880	5.180	5.270	...
Theory [40]	0.820	2.659	2.927	...	5.650	...
Theory [41]	0.800	2.709	3.076		5.590	
Exp. [56]				6.200		
Isosceles triangle $^2B_2$	E_b/n	r_1	r_2			
MP2	0.598	2.939	2.706			
MP4	0.695	2.932	2.711			
CCSD	0.642	2.961	2.721			
CCSD (T)	0.679	2.948	2.719			
Theory [27]	0.850	2.891	2.629			
Equilateral triangle $^2A_1'$	E_b/n		r			
MP2	0.579		2.836			
MP4	0.678		2.837			
CCSD	0.623		2.855			
CCSD (T)	0.662		2.849			
Linear structure $^2\Sigma_u^+$	E_b/n		r			
MP2	0.541		2.755			
MP4	0.632		2.748			
CCSD	0.609		2.781			
CCSD (T)	0.642		2.773			

Table 6. Binding energies per atom (in eV) and bond lengths (in Å) for different structures of Ag_3^+.

Equilateral triangle $^1A_1$	E_b/n	r
MP2	1.219	2.831
MP4	1.288	2.835
CCSD	1.237	2.849
CCSD (T)	1.263	2.845
Theory [34]	1.670	2.650
Theory [41]	1.247	2.804
Linear Structure $^1\Sigma_g$	E_b/n	r
MP2	0.794	2.799
MP4	0.917	2.801
CCSD	0.885	2.823
CCSD (T)	0.939	2.825

Table 7. Binding energies per atom (in eV) and bond lengths (in Å) for different structures of Ag_3^-.

Equilateral triangle $^3A_1'$	E_b/n	r
MP2	0.847	2.889
MP4	0.877	2.888
CCSD	0.838	2.923
CCSD (T)	0.871	2.913
Linear structure $^1\Sigma_g^+$	E_b/n	r
MP2	1.009	2.785
MP4	1.088	2.784
CCSD	1.023	2.806
CCSD (T)	1.063	2.798
Theory [28]	1.180	2.720
Theory [30]		2.760
Theory [41]		2.754

used. A possible reason for this insensitivity for MP theories, and to some extent for CC theories, might be the open shell nature of the Ag_3 cluster. The difference in binding energies between the isosceles and the equilateral structures are found to be 0.017 eV, 0.025 eV and 0.023 eV at the MP4, CCSD and CCSD (T) levels, respectively. For the trimer cation we have an equilateral triangle and for anion, a linear structure with the lowest possible multiplicities as the most stable structures. The linear structure of the anionic cluster is supported by experiments [16,17] as also by other theoretical calculations [30,41]. The binding energies increase as the level of theory changes from MP2 to MP4 and from CCSD to CCSD (T), with the equilateral trimer cation having higher binding energies than the linear trimer anion at every level of theory. For the equilateral cation, the positive charge is evenly distributed between the three atoms, which make this cluster more symmetrical electronically than the other two, hence higher binding energy. On the other hand, Mulliken charge analysis for the linear anion shows that excess negative charge is concentrated around the central atom, with the end atoms being relatively positively charged. The bond lengths for these structures are nearly equal to the bulk nearest-neighbor-distance of 2.89 Å [53].

For the silver tetramer, though it is generally accepted in the literature [30,31,33,34,42] that the rhombic structure is the most stable neutral structure, we investigated all five competing structures for determinations of relative stabilities at all four correlated levels of theory. Specifically, we studied a rhombus with D_{2h} symmetry, a square with D_{4h} symmetry, a linear geometry with $D_{\infty h}$ symmetry, a tetrahedron with T_d symmetry, and a T-shape with C_{2v} symmetry for the neutral, cationic and anionic tetramers. The clusters, as before, were constrained to have the geometries mentioned and bond lengths and angles were varied to arrive at the minimum energy structure and again all the clusters were spin-optimized. The optimized clusters are, as mentioned before, shown in Figure 1 and results are tabulated in Tables 8, 9, and 10, along with other published data in the literature. The rhombic

Table 8. Binding energies per atom, ionization potentials, electron affinities (all in eV), bond lengths (in Å) and bond angles (in degrees) for different structures of Ag_4.

Rhombus ^1A_g	E_b/n	r	α	AIP	VIP	EA
MP2	0.866	2.880	56.56	5.531	5.545	1.040
MP4	0.993	2.870	56.99	5.780	5.792	1.165
CCSD	0.907	2.890	56.88	5.615	5.636	1.084
CCSD (T)	1.079	2.886	57.00	5.722	5.735	1.164
Theory [30]	0.920	2.859	56.10		6.330	1.700
Theory [31]	1.100	2.740	57.20			
Theory [32]	1.219	2.630*	...	...	7.160	
Theory [33]	...	2.540	62.09		...	
Theory [34]	1.830	2.870	55.50		6.400	
Theory [35]	1.330	2.680	57.54	6.160	6.170	...
Theory [40]	1.210	2.731	56.60	...	6.860	...
Theory [41]	1.110	2.862	57.60		6.540	
Exp. [56]				6.650		
*estimated						
T-shape $^1A_1$	E_b/n	r_1	r_2	r_3		
MP2	0.797	2.700	2.920	2.710		
MP4	0.913	2.700	2.920	2.710		
CCSD	0.835	2.720	2.950	2.730		
CCSD (T)	0.879	2.716	2.938	2.723		
Theory [33]	...	2.600	2.800	2.610		
Theory [35]	1.250	2.510	2.650	2.550		
Square $^3A_{1g}$	E_b/n	r				
MP2	0.703	2.815				
MP4	0.810	2.818				
CCSD	0.739	2.834				
CCSD (T)	0.835	2.822				
Tetrahedron $^3A_2$	E_b/n	r				
MP2	0.509	2.910				
MP4	0.637	2.920				
CCSD	0.550	2.940				
CCSD (T)	0.623	2.944				
Linear $^1\Sigma_g^+$	E_b/n	r	a			
MP2	0.668	2.690	2.900			
MP4	0.874	2.740	2.740			
CCSD	0.761	2.760	2.760			
CCSD (T)	0.762	2.758	2.758			

structure was indeed found to be the most stable geometry for all the neutral, cationic and anionic cases studied. T-shape is the next possible structure for neutral Ag_4 at all levels of theory. However, the trend is not so clear between the other structures, *e.g.*, for neutral square and linear structure, the square has higher binding energy at MP2 and CCSD (T) level, whereas the linear structure is higher at MP4 and CCSD level. The difference in binding energies per atom between the neutral rhombic structure and the T-shape is 0.080 eV at the MP4 level and 0.200 eV at the CCSD (T) level. The corresponding differences are 0.026 eV and 0.027 eV for the cation. For the anion, the differences are 0.070 eV and 0.031 eV. Liu *et al.* [33] have indicated that as temperature increases

Table 9. Binding energies per atom (in eV), bond lengths (in Å), and bond angles (in degrees) for different structures of Ag_4^+.

Rhombus $^2B_{1u}$	E_b/n	r	α	
MP2	1.135	2.920	56.85	
MP4	1.214	2.920	57.07	
CCSD	1.159	2.940	56.92	
CCSD (T)	1.193	2.930	57.05	
Theory [35]	1.560	2.700	58.05	
Theory [41]	...	2.909	57.40	
T-shape $^2A_1$	E_b/n	r_1	r_2	r_3
MP2	1.119	2.900	2.850	2.780
MP4	1.188	2.890	2.860	2.790
CCSD	1.139	2.910	2.880	2.800
CCSD (T)	1.166	2.896	2.875	2.798
Theory [35]	1.510	2.600	2.640	2.610
Square $^2A_{1g}$	E_b/n	r		
MP2	0.631	3.087 ($^4A_{1g}$)		
MP4	1.031	2.830		
CCSD	0.977	2.850		
CCSD (T)	1.015	2.852		
Tetrahedron $^2A_1$	E_b/n	r		
MP2	1.036	2.919		
MP4	1.119	2.920		
CCSD	1.056	2.930		
CCSD (T)	1.093	2.935		
Linear $^2\Sigma_u^+$	E_b/n	r	a	
MP2	0.871	2.840	2.840	
MP4	0.924	2.830	2.830	
CCSD	0.927	2.850	2.850	
CCSD (T)	0.955	2.827	2.827	

Table 10. Binding energies per atom (in eV), bond lengths (in Å), and bond angles (in degrees) for different structures of Ag_4^-.

Rhombus $^2B_{2u}$	E_b/n	r	α	
MP2	1.059	2.860	61.05	
MP4	1.139	2.860	59.26	
CCSD	1.041	2.880	59.22	
CCSD (T)	1.099	2.890	60.35	
Theory [30]		2.849	61.20	
Theory [41]		2.852	63.70	
T-shape $^2B_2$	E_b/n	r_1	r_2	r_3
MP2	0.981	2.730	2.880	2.860
MP4	1.069	2.710	2.870	2.850
CCSD	1.022	2.770	2.910	2.890
CCSD (T)	1.068	2.770	2.898	2.889
Theory [30]		2.730	2.850	2.872
Square ^2B_u	E_b/n	r		
MP2	1.059	2.861		
MP4	1.022	2.830		
CCSD	0.932	2.860		
CCSD (T)	0.992	2.855		
Tetrahedron $^4A_1$	E_b/n	r		
MP2	0.773	2.911		
MP4	0.855	2.920		
CCSD	0.763	2.950		
CCSD (T)	0.842	2.955		
Linear $^2\Sigma_g^+$	E_b/n	r	a	
MP2	0.961	2.770	2.840	
MP4	1.028	2.770	2.770	
CCSD	1.012	2.810	2.810	
CCSD (T)	1.052	2.827	2.808	
Theory [30]		2.840	2.780	

rhombic and T-shape may become isomers. One structure may transform into another by thermal fluctuation.

We also considered the highly symmetrical tetrahedral T_d structure as a possibility of a three dimensional structure for the silver tetramer. The valence electrons are insufficient to fill the degenerate one-electron levels of the tetrahedral structure and Jahn-Teller deformation causes it not being the most stable structure [28]. In fact, the triplet state was found to have higher binding energy than the singlet for the neutral tetrahedron. Anions are also at higher spin state with multiplicity four, while cations are in doublet state. Except for the cationic tetramer, the binding energies per atom are much less than the rhombic structures. For the cation at the MP4 level, the tetrahedron is 0.095 eV lower than the rhombic structure, and at the CCSD (T) level the difference is 0.100 eV. For the anion, a competing structure is the linear structure. At the MP4 level, the binding energies per atom between the rhombic and the linear structures differ by 0.111 eV, while at the CCSD (T) level, the difference is 0.047 eV. The all-electron spin density calculations of Kaplan *et al.* [30], on the other hand, found a large difference of 0.460 eV between these two anionic structures. The charge distribution on the neutral rhombic and square clusters is symmetric with diagonally opposite atoms having charges of the same sign, but in the square the magnitude of charges on each atom is almost twice than the rhombic structure (Tab. 16). This makes the overall binding energy of square structure much lower than the rhombic structure. Due to Jahn-Teller deformation, the triplet state was found to be more bounded than the singlet at all four levels of theories. For the cations, only the MP2 level of theory showed that the state with multiplicity four was more bounded, but the other three levels of theories found the doublet state to be more favorable. For the anion, all four levels of theory indicated the ground state structure to be a doublet.

In general, our results indicate that the binding energies follow the trend $E_b(\mathrm{MP4}) > E_b(\mathrm{CCSD\,(T)}) > E_b(\mathrm{CCSD}) > E_b(\mathrm{MP2})$ (Figs. 2–4). This pattern is not obeyed for the silver dimer anion, where the coupled

cluster theories produce higher binding energies compared to the perturbation theory eigenvalues. For the neutral silver tetramer, CCSD (T) binding energy is higher than the MP4 binding energy and the CCSD (T) AIP is closer to the experimental value compared to the MP4 AIP value. As a general feature for the clusters considered here, the cationic bond lengths are slightly greater than the neutral or anionic bond lengths, which may be due to the loss of one bonding *s*-electron. Kresin [54] has observed that for Ag cationic clusters the electron spill out is rather weak, which implies higher electron densities, hence higher binding energies than the anions and neutrals. Our data support this fact. As it is well-known that for smaller clusters *d*-orbitals are more localized than the *s*-orbitals, so the bondings are mainly due to *s*-orbitals. A slight increase in the molecular orbital coefficients for *d*-electrons was found for Ag_n as n goes from 2 to 4.

The ionization potentials, adiabatic and vertical, as a function of cluster size are shown in Figures 5 and 6, respectively. The expected saw-tooth behavior is indicated by the higher IPs at Ag_2 and Ag_4. To ionize these two clusters, closed-shell has to be broken to form open-shells $^2\Sigma_g^+$ and $^2B_{1u}$ respectively. The lowest value of IP for Ag_3 is justified because, ionization leads to the formation of a closed-shell $^1A_1$ electronic state, which makes Ag_3^+ as the most symmetrically stable cluster compared to the other cations. However, our values are lower than the experimental values and comparisons with other theoretical results are presented in Tables 2, 5, and 8. The AIP values quoted by Bonacic-Koutecky *et al.* [35] are systematically higher than our values but still less than the experimental values. The difference in the molecular orbital coefficients between neutral and cationic clusters is not negligible which means that the relaxation error is significant. This also means that the Koopman's theorem [47] does not predict good estimates of IPs in these cases. Electron affinities (EA) were also calculated for the all the clusters and are presented as a function of cluster size in Figure 7. We observed the same alternating behavior as predicted by experiment [14] and clusters with lower ionization potentials are found to have higher electron affinities. Again, the theoretical electron affinities are lower compared to experimental values. It is quite possible that the low theoretical values of the ionization potentials and electron affinities are merely an artifact of the pseudopotential and the size of the basis set, and are not due to any fundamental effects. The EAs calculated by Kaplan *et al.* [30] are closer to the experimental values (Fig. 7). These affinities were calculated with neutral clusters having identical structures as the anions.

We also computed the fragmentation energies of the optimized clusters into different possible binary channels. These energies were computed from

$$E_{n\to(n-m)+m} = E_{n-m} + E_m - E_n, \qquad n > m \leq 1, \quad (6)$$

for the channel $Ag_n \to Ag_{n-m} + Ag_m$, where E_n is the total energy of the corresponding stable structure. The values are summarized in Tables 11–14. In general, the preferred channel of decay is the most symmetrical channel.

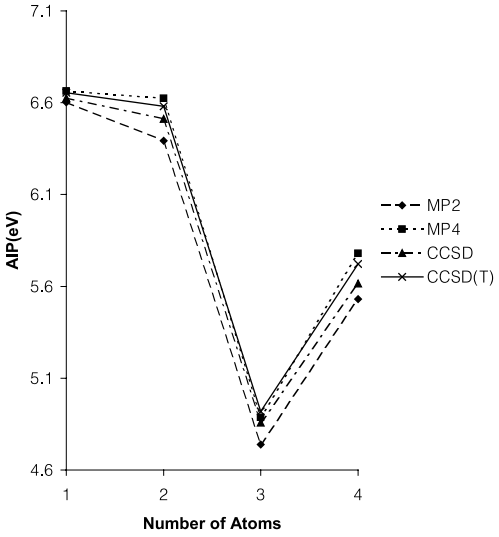

Fig. 5. Adiabatic ionization potentials of silver clusters *vs.* number of atoms in the cluster.

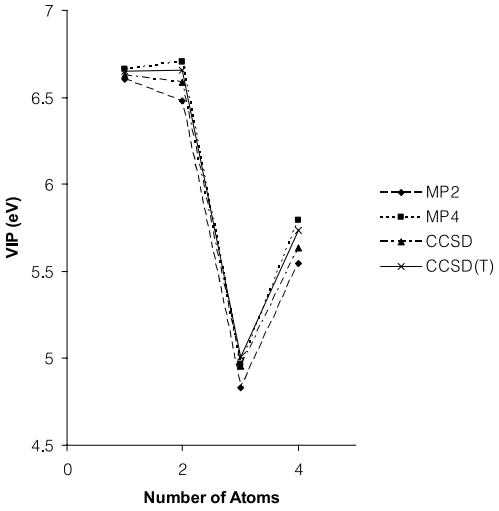

Fig. 6. Vertical ionization potentials of silver clusters *vs.* number of atoms in the cluster.

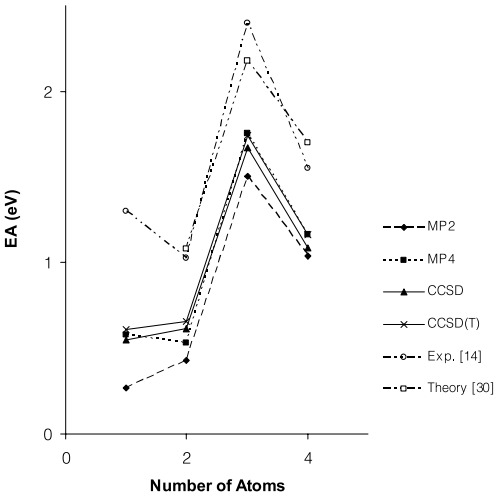

Fig. 7. Electron affinities of silver clusters *vs.* number of atoms in the cluster.

Table 11. Fragmentation energies (in eV) at MP2 level of silver clusters.

Final Clusters	Initial clusters								
	Ag_2	Ag_3	Ag_4	Ag_2^+	Ag_3^+	Ag_4^+	Ag_2^-	Ag_3^-	Ag_4^-
Ag	1.818	0.611	1.673	1.391	2.266	0.881	1.342	1.687	1.209
Ag_2		0.611	1.104		2.476	1.966		1.848	1.715
Ag_3			1.673			2.746			2.445

Table 12. Fragmentation energies (in eV) at MP4 level of silver clusters.

Final clusters	Initial clusters								
	Ag_2	Ag_3	Ag_4	Ag_2^+	Ag_3^+	Ag_4^+	Ag_2^-	Ag_3^-	Ag_4^-
Ag	1.379	0.710	1.880	1.420	2.440	0.990	1.330	1.930	1.29
Ag_2		0.710	1.210		2.480	2.050		1.88	1.845
Ag_3			1.880			2.770			2.740

Table 13. Fragmentation energies (in eV) at CCSD level of silver clusters.

Final clusters	Initial clusters								
	Ag_2	Ag_3	Ag_4	Ag_2^+	Ag_3^+	Ag_4^+	Ag_2^-	Ag_3^-	Ag_4^-
Ag	1.289	0.691	1.684	1.404	2.308	0.927	1.355	1.714	1.095
Ag_2		0.691	1.045		2.423	1.946		1.779	1.556
Ag_3			1.684			2.695			2.263

Table 14. Fragmentation energies (in eV) at CCSD (T) level of silver clusters.

Final clusters	Initial clusters								
	Ag_2	Ag_3	Ag_4	Ag_2^+	Ag_3^+	Ag_4^+	Ag_2^-	Ag_3^-	Ag_4^-
Ag	1.342	0.713	1.783	1.415	2.374	0.982	1.392	1.797	1.206
Ag_2		0.713	1.154		2.533	2.013		1.847	1.660
Ag_3			1.783			2.716			2.339

Specifically, we comment on the decay channel of the silver tetramer. Though the binding energy per atom for neutral Ag_2 and Ag_3 are almost same, the most probable end product of decaying Ag_4 is (Ag_2 + Ag_2) cluster, not (Ag_3 + Ag). This has been observed also before by us for the V_4 cluster [55]. For ionic clusters, charge is usually carried out by the larger clusters, for example, for tetramer cation, the dominant decay channel is (Ag_3^+ + Ag). However, for the anionic trimer, the most favorable decay channel is (Ag_2 + Ag^-) at the MP4 level, in agreement with experimental data [14]. The other levels of theories however predict the channel $Ag_3^- \rightarrow Ag + Ag_2^+$. For Ag_4^+, (Ag_3^- + Ag) is the favorable decay mode at all levels of theories, again in agreement with experimental results [14]. The bond dissociation energies, defined by the energy needed to break a cluster Ag_n into Ag_{n-1} and Ag, have also alternating behavior with higher values at Ag_2 and Ag_4.

To ensure that the optimized structures obtained do indeed represent global minima, and are not local minima, we also computed the harmonic frequencies at each optimized geometric configuration. As has been pointed out by Poteau *et al.* [31], experimental determinations of the frequencies could help identify cluster structures produced in beams. The MP2 results are shown in Table 15. For the dimer, we computed the frequencies at the MP4 and the CCSD levels also and note that the values are fairly close together at the different levels of theory. However, all the theoretically calculated frequencies are lower than the experimental frequency. The MP2 value is closest to the experimental value, the percent difference being fifteen percent. Also, all the frequencies are positive and in general, the ionic clusters have lower vibrational frequencies compared to those for the neutral clusters. The cationic dimer MP2 frequency is also lower than the experimental value, the percent difference being seventeen percent. In Table 15, the neutral cluster frequencies are also compared with the results of Poteau *et al.* [31], in which, except for Ag_2, the frequencies were calculated using a tight-binding model fitted on the DFT results. Except for two values, the frequencies of Poteau *et al.* are consistently higher than the frequencies obtained by us, the percent difference ranging from thirteen percent to forty percent.

In summary, the formalisms of many body perturbation theory and coupled cluster theory have been used to study the electronic and geometric structures of neutral, cationic, and anionic small silver clusters. Topologically different clusters and clusters belonging to different symmetry groups have been identified and studied in detail. Full geometry optimizations have been carried out at four different correlated levels of theories. Ionization potentials, electron affinities, and fragmentation energies of the optimized clusters have been compared with other experimental and theoretical results available in the

Table 15. Harmonic frequencies (in cm^{-1}) of the most stable silver clusters computed at MP2 level.

Ag_4	Ag_4^+	Ag_4^-	Ag_3	Ag_3^+	Ag_3^-	Ag_2	Ag_2^+	Ag_2^-
32.50	13.8	29.48	58.84	106.74	37.48	163.63	112.44	125.22
(23.30)			(70.9)			(185.1)	[135.8]	
75.36	69.25	81.97	64.16	106.74	37.48	161.87(MP4)		
(90.0)			(90.4)					
81.48	85.24	93.36	167.47	156.85	98.73	157.50(CCSD)		
(106.6)			(170.0)					
97.65	85.58	103.75			165.24	[192.4]		
(110.2)								
147.55	112.78	139.53						
(140.1)								
166.13	154.03	144.76						
(181.3)								

Table 16. Mulliken charge distributions for ground state Ag clusters at optimized geometries.

Clusters	Atom	Charge			
		MP2	MP4	CCSD	CCSD (T)
Ag_2	1	0.000	0.000	0.000	0.000
	2	0.000	0.000	0.000	0.000
Ag_2^+	1	0.500	0.500	0.500	0.500
	2	0.500	0.500	0.500	0.500
Ag_2^+	1	−0.500	−0.500	−0.500	−0.500
	2	−0.500	−0.500	−0.500	−0.500
Ag_3	1	0.126	0.282	0.282	0.142
	2	−0.063	−0.141	−0.141	−0.071
	3	−0.063	−0.141	−0.141	−0.071
Ag_3^+	1	0.333	0.333	0.333	0.333
	2	0.333	0.333	0.333	0.333
	3	0.333	0.333	0.333	0.333
Ag_3^-	1	−1.099	−1.159	−1.163	−1.194
	2	0.049	0.079	0.081	0.097
	3	0.049	0.079	0.081	0.097
Ag_4	1	−0.004	−0.099	−0.096	−0.098
	2	0.004	0.099	0.096	0.098
	3	−0.004	−0.099	−0.096	−0.098
	4	0.004	−0.099	0.096	0.098
Ag_4^+	1	0.214	0.342	0.341	0.341
	2	0.286	0.158	0.159	0.159
	3	0.214	0.342	0.340	0.341
	4	0.286	0.158	0.160	0.159
Ag_4^+	1	−0.278	−0.167	−0.216	−0.343
	2	−0.221	−0.333	−0.284	−0.157
	3	−0.278	−0.167	−0.216	−0.343
	4	−0.221	−0.333	−0.284	−0.157

literature. All levels of correlated theories appear to perform well for small silver clusters in that no convergence problems are encountered at the various levels of theories. This is noteworthy since it has been claimed [21,22] that for d elements the MP series does not converge very well.

The authors gratefully acknowledge partial support from the Welch Foundation, Houston, Texas (Grant No. Y-1525).

References

1. S. Bjornholm, J. Borggreen, Phil. Mag. B **79**, 1321 (1999)
2. P. Jena, S.N. Khanna, B.K. Rao, *Theory of Atomic and Moleculer Clusters* (Springer-Verlag, Berlin, 1999), pp. 27-53
3. U. Naher, S. Bjornholm, S. Frauendorf, F. Garcias, C. Guet, Phys. Rep. **285**, 245 (1997)
4. J. Yoon, K.S. Kim, K.K. Baek, J. Chem. Phys. **112**, 9335 (2000), and references therein
5. S. Kruckeberg, G. Dietrich, K. Lutzenkirchen, L. Schweikhard, C. Walther, J. Ziegler, Eur. Phys. J. D **9**, 169 (1999)
6. Y. Shi, V.A. Spasov, K.M. Ervin, J. Chem. Phys. **111**, 938 (1999)
7. M. Lindinger, K. Dasgupta, G. Dietrich, S. Kruckeberg, S. Kuznetsov, K. Lutzenkirchen, L. Schweikhard, C. Walther, J. Ziehler, Z. Phys. D **40**, 347 (1997)
8. T.L. Haslett, K.A. Bosnick, M. Moskovits, J. Chem. Phys. **108**, 3453 (1998)
9. I. Rabin, C. Jackschath, W. Schulze, Z. Phys. D **19**, 153 (1991)
10. S. Kruckeberg, G. Dietrich, K. Lutzenkirchen, L. Schweikhard, C. Walther, J. Ziehler, Z. Phys. D **40**, 341 (1997)
11. S. Kruckeberg, G. Dietrich, K. Lutzenkirchen, L. Schweikhard, C. Walther, J. Ziegler, Eur. Phys. J. D **9**, 145 (1999)
12. K.A. Bosnick, T.L. Haslett, S. Fedrigo, M. Moskovits, W.-T. Chan, R. Fournier, J. Chem. Phys. **111**, 8867 (1999)
13. D. Salz, R. Lamber, M. Wark, A. Baalmann, N. Jaeger, Phys. Chem. Chem. Phys. **1**, 4474 (1999)
14. V.A. Spasov, T.H. Lee. J.P. Maberry, K.M. Ervin, J. Chem. Phys. **110**, 5208 (1999), and references therein
15. H. Handschuh, C.-Y. Cha, P.S. Bechthold, G. Gantefor, W. Eberhardt, J. Chem. Phys. **102**, 6406 (1995)
16. T. Leisner, S. Vajda, S. Wolf, L. Woste, J. Chem. Phys. **111**, 1017 (1999)
17. D.W. Boo, Y. Ozaki, L.H. Andersen, W.C. Lineberger, J. Phys. Chem. A **101**, 6688 (1997)

18. K. Yabana, G.F. Bertsch, Phys. Rev. A **60**, 3809 (1999)
19. D.-A. Luh, J.J. Paggel, T. Miller, T.-C. Chiang, Phys. Rev. Lett. **84**, 3410 (2000)
20. A.A. Bagatur'yants, A.A. Safonov, H. Stoll, H.-J. Werner, J. Chem. Phys. **109**, 3096 (1998)
21. K. Raghavachari, G.W. Trucks, J. Chem. Phys. **91**, 1062 (1989)
22. M. Seth, F. Cooke, P. Schwerdtfeger, J.-L. Heully, M. Pelissier, J. Chem. Phys. **109**, 3935 (1998)
23. R.P. Gupta, Phys. Rev. B **23**, 6265 (1981)
24. V. Rosato, G. Guillope, B. Legrand, Phil. Mag. A **50**, 321 (1998)
25. A.P. Sutton, *Electronic Structure of Materials* (Oxford University Press, 1993)
26. K. Michaelin, N. Rendon, I.L. GarZon, Phys. Rev. B **60**, 2000 (1999)
27. V. Bonacic-Koutecky, L. Cespiva, P. Fantucci, J. Kouteckey, J. Chem. Phys. **98**, 7981 (1993)
28. V. Bonacic-Koutecky, L. Cespiva, P. Fantucci, J. Pittner, J. Koutecky, J. Chem. Phys. **100**, 490 (1994)
29. S. Fedrigo, W. Harbich, J. Buttet, Phys. Rev. B **47**, 10706 (1993)
30. I.G. Kaplan, R. Santamaria, O. Novaro, Int. J. Quant. Chem. **S27**, 743 (1993); R. Santamaria, I.G. Kaplan, O. Novaro, Chem. Phys. Lett. **218**, 395 (1994)
31. R. Poteau, J.-L. Heully, F. Spiegelmann, Z. Phys. D **40**, 479 (1997)
32. R. Fournier, J. Chem. Phys. **115**, 2165 (2001)
33. Z.F. Liu, W.L. Yim, J.S. Tse, J. Henfer, Eur. Phys. J. D **10**, 105 (2000)
34. K. Balasubramanian, M.Z. Liao, Chem. Phys. **127**, 313 (1988); K. Balasubramanian, P.Y. Feng, Chem. Phys. Lett. **159**, 452 (1989); J. Phys. Chem. **94**, 1536 (1990)
35. V. Bonacic-Koutecky, J. Pittner, M. Boiron, P. Fantucci, J. Chem. Phys. **110**, 3876 (1999)
36. V.G. Kuznefson, I.V. Abarenkov, V.A. Batuev, A.V. Titov, I.I.Tupitsyn, N.S. Mosyagin, Opt. Spek. **84**, 357 (1999)
37. P.J. Hay, W.R. Wadt, J. Chem. Phys. **82**, 270 (1985)
38. A. Ramirez-Solis, V. Vallet, C. Teichteil, T. Leininger, J.P. Daudey, J. Chem. Phys. **115**, 3201 (2001)
39. E.A.A. Jarvis, E. Fattal, A.J.R. da Silva, E.A. Carter, J. Phys. Chem. A **104**, 2333 (2000)
40. J. Zhao, Y. Luo, G. Wang, Eur. Phys. J. D **14**, 309 (2001)
41. H. Partridge, C.W. Bauschlicher Jr, S.R. Langhoff, Chem. Phys. Lett. **175**, 531 (1990); C.W. Bauschlicher Jr, S.R. Langhoff, H. Partridge, J. Chem. Phys. **91**, 2412 (1989); C.W. Bauschlicher Jr, S.R. Langhoff, H. Partridge, J. Chem. Phys. **93**, 8133 (1990)
42. M. Head-Gordon, T. Head-Gordon, Chem. Phys. Lett. **220**, 122 (1994); S. Saebo, J. Almlof, Chem. Phys. Lett. **154**, 83 (1989)
43. R. Krishnan, J.A. Pople, Int. J. Quant. Chem. **14**, 91 (1978)
44. G.D. Purvis, R.J. Bartlett, J. Chem. Phys. **76**, 1910 (1982); J.A. Pople, M. Head-Gordon, K. Raghavachari, J. Chem. Phys. **87**, 5968 (1987); G.E. Scuseria, H.F. Schaefer III, J. Chem. Phys. **90**, 3700 (1989)
45. J. Goldstone, Proc. Roy. Soc. Lond. A **239**, 267 (1956)
46. P.O. Lowdin, J. Math. Phys. **6**, 1341 (1965); Phys. Rev. A **139**, 357 (1965)
47. A. Szabo, N.S. Ostlund, *Modern Quantum Chemistry* (Macmillan, New York, 1982)
48. T.D. Crawford, H.F. Schaefer III, in *Reviews in Computational Chemistry*, edited by K.B. Lipkowitz, D.B. Boyd (John Wiley and Sons, New York, 2000), Vol. 14, p. 33
49. W.J. Hehre, P.v.R. Schleyer, J.A. Pople, *Ab Initio Molecular Orbital Theory* (Wiley, New York, 1982)
50. P.J. Hay, W.R. Wadt, J. Chem. Phys. **82**, 299 (1985)
51. C.E. Moore, Atomic Energy levels, Circ. No. 467, Nat. Bur. Standards, Vol. III, 1958
52. *Gaussian 98* (Revision A.1), M.J. Frisch, G.W. Trucks, H.B. Schlegel, G.E. Scuseria, M.A. Robb, J.R. Cheeseman, V.G. Zakrzewski, J.A. Montgomery, R.E. Stratmann, J.C. Burant, S. Dapprich, J.M. Millam, A.D. Daniels, K.N. Kudin, M.C. Strain, O. Farkas, J. Tomasi, V. Barone, M. Cossi, R. Cammi, B. Mennucci, C. Pomelli, C. Adamo, S. Clifford, J. Ochterski, G.A. Petersson, P.Y. Ayala, Q. Cui, K. Morokuma, D.K. Malick, A.D. Rabuck, K. Raghavachari, J.B. Foresman, J. Cioslowski, J.V. Oritz, B.B. Stefanov, G. Liu, A. Liashenko, P. Piskorz, I. Komaromi, R. Gomperts, R.L. Martin, D.J. Fox, T. Keith, M.A. Al-Laham, C.Y. Peng, A. Nanayakkara, C. Gonzalez, M. Challacombe, P.M.W. Gill, B.G. Johnson, W. Chen, M.W. Wong, J.L. Andres, M. Head-Gordon, E.S. Replogle, J.A. Pople, Gaussian Inc., Pittsburgh PA, 1998
53. C. Kittel, *Introduction to Solid State Physics* (John Wiley and Sons, New York, 1996)
54. V.V. Kresin, Phys. Rev. B **51**, 1844 (1995)
55. X. Wu, A.K. Ray, J. Chem. Phys. **110**, 2437 (1999)
56. C. Jackschath, I Rabin, W. Schulze, Z. Phys. D **22**, 517 (1992)
57. M.D. Morse, Chem. Rev. **86**, 1049 (1986)
58. V. Beutel, G.L. Bhale, M. Kuhn, W. Demtroder, Chem. Phys. Lett. **185**, 313 (1991)